Sensitivity Considerations in Microwave Paramagnetic Resonance Absorption Techniques

By G. FEHER

(Manuscript received February 9, 1956)

This paper discusses some factors which limit the sensitivity of microwave paramagnetic resonance equipments. Several specific systems are analyzed and the results verified by measuring the signal-to-noise ratio with known amounts of a free radical. The two most promising systems, especially at low powers, employ either superheterodyne detection or barretter homodyne detection. A detailed description of a superhetrodyne spectrometer is given.

TABLE OF CONTENTS

I. INTRODUCTION

Within the past few years the field of paramagnetic resonance absorption has become an important tool in physical and chemical research. In many ways its usefulness is limited by the sensitivity of the experimental set up. A typical example is the study of semiconductors in which case one would like to investigate as small a number of impurities as possible. It is the purpose of this paper to analyze the sensitivity limits of several experimental set ups under different operating conditions. This was done in the hope that an understanding of these limitations would put one in a better position to design a high sensitivity electron spin resonance equipment. In the last section the performance of the different experimental arrangements is tested. The agreement obtained with the predicted performance proves the essential validity of the analysis. This paper is primarily for experimental physicists confronted with the problem of setting up a high sensitivity spectrometer.

II. GENERAL BACKGROUND

We will not consider here the detailed theory[1] of the resonance phenomenon but consider this part of the problem only from a phenomenological point of view. When a paramagnetic sample is placed into an RF field of amplitude H_1 of a frequency ω at right angles to which there is a dc magnetic field H_0, magnetic dipole transitions will be induced in the neighborhood of the resonance condition

$$h\omega = g\beta H_0 \tag{1}$$

where g is the spectroscopic splitting factor, h is Planck's constant and β is the Bohr magneton. As a result of these transitions power will be absorbed from the microwave field H_1. This power absorption is associated with the imaginary part of the RF susceptibility χ''. The transmitted (or reflected) H_1 will also experience a phase shift which is associated with the real part of the RF susceptibility χ'. The sensitivity of the setup is then determined by how small a power absorption (or phase shift) one is able to detect when going through a resonance

III. Q CHANGES ASSOCIATED WITH THE ABSORPTION

The average power absorbed per unit volume of a paramagnetic sample is

$$P = \tfrac{1}{2}\omega H_1^2 \chi'' \tag{2}$$

For low enough powers χ'' is not a function of H_1 (and even for very high powers never drops off faster than $1/H_1^2$), so that for a large power absorption one would like a large RF magnetic field. This suggests a resonant cavity which indeed is used in all experimental setups. The Q of a cavity into which a paramagnetic sample is placed is given by

$$Q = \omega \frac{\text{Energy Stored}}{\text{Average Power Dissipated}} = \omega \frac{\frac{1}{8\pi}\int_{V_c} H_1^2\, dV_c}{P_1 + \frac{1}{2}\omega \int_{V_s} H_1^2 \chi''\, dV_s} \tag{3}$$

where P_1 = power dissipated in the cavity in the absence of any paramagnetic losses, V_s is the sample volume and V_c the cavity volume.

Assuming that the paramagnetic losses are small in comparison with P_1 we get

$$Q = Q_0 \left(1 - 4\pi \frac{\int_{V_s} H_1^2 \chi''\, dV_s}{\int_{V_c} H_1^2\, dV_c} Q_0 \right) = Q_0(1 - 4\pi\chi''\eta Q_0) \tag{4}$$

$$\therefore \Delta Q = Q_0^2 4\pi\chi''\eta$$

where Q_0 is the cavity Q in the absence of paramagnetic losses and η is the filling factor and depends on the field distribution in the cavity and the sample. For example, in a rectangular cavity excited in the TE_{101} mode

$$\eta = \frac{V_s}{V_c} \frac{4}{1 + \left(\frac{d}{a}\right)^2} \tag{5}$$

where d is the length of the cavity and a the width along which the E field varies. In the above example it was assumed that the sample is small in comparison to a wavelength and is placed in the max. H_1 field.

IV. COUPLING TO RESONANT CAVITIES FOR MAXIMUM OUTPUT

Having established the Q changes associated with the resonance absorption, we will next determine the proper coupling to the resonant cavity in order that the Q changes result in a maximum change in transmitted or reflected power (or voltage). The derivation will be based on the assumption that we have a fixed amount of power available from our source and that the Q change is not a function of the RF power (no saturation effects).

A. Reflection Cavity

Fig. 1 shows a magic (hybrid) T which serves to observe the reflected power from the cavity. Arm 3 has a slide screw tuner which serves to balance out some of the power coming from arm 2. This does not affect the present analysis and will be considered later in connection with detector noise. It should be mentioned, however, that a certain amplitude or phase unbalance has to be left. This insures that the signal in arm 4 will be a function of either χ' or χ''.[1] In the case that the magic T is completely balanced out the signal in arm 4 will be a function of both χ' and χ'' and the experimental results become difficult to analyze.

Fig. 2 shows the equivalent circuit for a reflection cavity.[2] The $\sqrt{2}$ in the source voltage arises from the fact that half the power is lost in arm 3. From this equivalent circuit we can define the following relations:

$$\text{Unloaded } Q = Q_0 = \frac{\omega L}{r} \text{ (Losses due to cavity alone)} \tag{6}$$

$$\text{External } Q = Q_x = \frac{\omega L}{R_0 n^2} \text{ (Losses arising from power leaking out of the cavity)} \tag{7}$$

$$\text{Loaded } Q = Q_L = \frac{\omega L}{R_0 n^2 + r} \text{ (Losses due to both cavity and leakage out)} \tag{8}$$

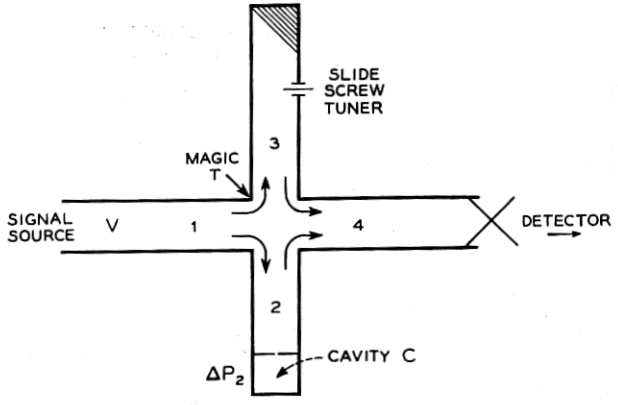

Fig. 1 — A simple arrangement to observe the reflected power from cavity C.

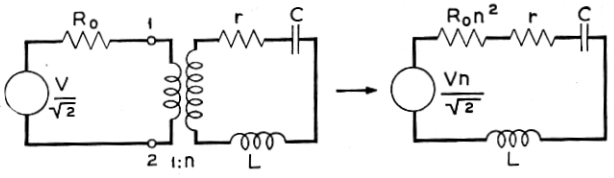

Fig. 2 — Equivalent circuit for a reflection cavity.

We define the coupling coefficient $\beta = Q_x/Q_0$ such that:

$$\text{Critically coupled cavity } \beta = \frac{Q_0}{Q_x} = \frac{R_0 n^2}{r} = 1 \tag{9}$$

$$\text{Overcoupled cavity } \frac{Q_0}{Q_x} > 1 \qquad \text{VSWR} = \beta = \frac{R_0 n^2}{r} \tag{10}$$

$$\text{Undercoupled cavity } \frac{Q_0}{Q_x} < 1 \qquad \text{VSWR} = \frac{1}{\beta} = \frac{r}{R_0 n^2} \tag{11}$$

We will see that the coupling coefficient for maximum output depends on the characteristics of the detecting element. Two cases will be treated: the power (square law) detector and the voltage (linear) detector.

1. Detector Output Proportional to Incident Power

Power into the cavity at resonance

$$P_c = \left(\frac{Vn}{\sqrt{2}}\right)^2 \frac{r}{(R_0 n^2 + r)^2}$$

Max. power available from source (in arm 1)

$$P_0 = \frac{(Vn)^2}{4R_0 n^2} \quad \therefore \; P_c = P_0 \frac{2R_0 n^2 r}{(R_0 n^2 + r)^2}$$

The change in reflected power ΔP_R equals the change in the power inside the cavity ΔP_c (since the incident power stays the same).

$$\Delta P_c = \frac{\partial P_c}{\partial r} \Delta r = 2R_0 n^2 P_0 \frac{R_0 n^2 - r}{(R_0 n^2 + r)^3} \Delta r \tag{12}$$

We want to optimize ΔP_c with respect to the coupling parameter n^2 (or $R_0 n^2$), i.e.,

$$\frac{\partial(\Delta P_c)}{\partial(R_0 n^2)} = (R_0 n^2)^2 - 4(R_0 n^2) r + r^2 = 0$$

$$\therefore \frac{R_0 n^2}{r} = 2 \pm \sqrt{3} \tag{13}$$

the positive sign being associated with the overcoupled, the negative with the undercoupled case. The experimentally measured quantity is the voltage standing wave ratio VSWR $= 2 + \sqrt{3} = 3.74$ corresponding to a reflection coefficient of 0.58. Putting this value into (12) we get for the maximum signal

$$\frac{\Delta P_c}{P_0} = \pm\, 0.193 \frac{\Delta r}{r} = \mp\, 0.193 \frac{\Delta Q_0}{Q_0} = \mp\, (0.193)(4\pi)\chi'' \eta Q_0 \tag{14}$$

the last step being obtained with the aid of (4). Equation (12) is plotted in Fig. 4. From the symmetry of the graph it is obvious that for a given VSWR, the signal will be the same for the overcoupled and undercoupled case. However, as we will see later from the standpoint of noise the 2 cases are not necessarily identical.

2. Detector Output Proportional to Input Voltage

Let Γ be the reflection coefficient, then V_{REFL} from the cavity is

$$V_{\text{REFL}} = \frac{V}{\sqrt{2}}\Gamma = \frac{V}{\sqrt{2}}\left(\frac{\text{VSWR} - 1}{\text{VSWR} + 1}\right) = -\frac{V}{\sqrt{2}}\left[1 - \frac{2\text{VSWR}}{\text{VSWR} + 1}\right]$$

With the aid of (10) and (11) this gives for the undercoupled case:

$$V_{\text{REFL}} = -\frac{V}{\sqrt{2}}\left(1 - \frac{2r}{R_0n^2 + r}\right)$$

and the overcoupled case

$$V_{\text{REFL}} = -\frac{V}{\sqrt{2}}\left(1 - \frac{2R_0n^2}{R_0n^2 + r}\right)$$

We are interested only in the change of output voltage which is:

$$\Delta V_{\text{REFL}} = \frac{\partial V_{\text{REFL}}}{\partial r}\Delta r = \pm\sqrt{2}\,V\Delta r\,\frac{R_0n^2}{(R_0n^2 + r)^2} \tag{15}$$

The two signs corresponding to the undercoupled or overcoupled case, respectively. In order to find the optimum coupling

$$\frac{\partial(\Delta V)}{\partial(R_0n^2)} = R_0n^2 - r = 0$$

$$\therefore \frac{R_0n^2}{r} = 1$$

Putting this value into (15) we get the max. value

$$\frac{\Delta V_{\text{REFL}}}{V} = \pm\frac{\sqrt{2}}{4}\frac{\Delta r}{r} = \mp\frac{\sqrt{2}}{4}\frac{\Delta Q_0}{Q_0} = \mp\frac{\sqrt{2}}{4}4\pi\chi''\eta Q_0 \tag{16}$$

(15) is again plotted in Fig. 4. From this graph we see that for maximum sensitivity we want to work near match. However, one should not work so close to match that the absorption signal will carry the cavity through the matching condition while sweeping through a resonance line. This would result (due to the sign reversal of the signal at match) in a distorted line. Incidentally, the sign of the signal may be conveniently used

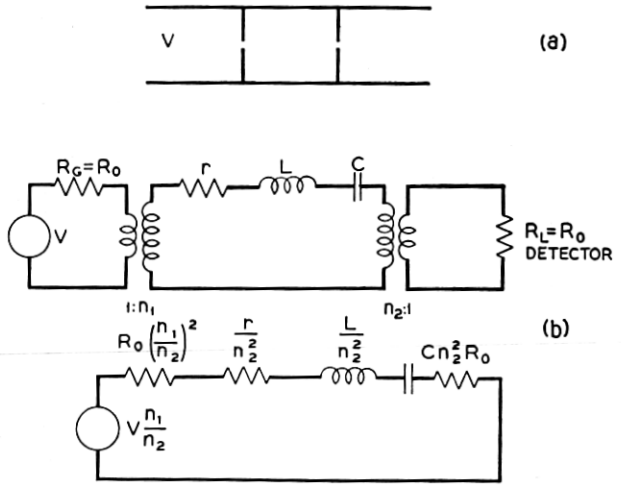

Fig. 3 — Equivalent circuit for a transmission cavity.

to determine whether the cavity is overcoupled or undercoupled. This information may be necessary in Q_0 determinations.[12]

B. Transmission Cavity

Fig. 3 shows the equivalent circuit for a transmission cavity,[2] the generator and the detector being matched to the waveguide, i.e.,

$$R_G = R_L = R_0$$

Analogous to the reflection cavity we define again two coupling coefficients

$$\beta_1 = \frac{R_0 n_1^2}{r} \qquad \beta_2 = \frac{R_0 n_2^2}{r} \tag{18}$$

the relation between the unloaded and loaded Q being

$$Q_0 = Q_L(1 + \beta_1 + \beta_2) \tag{19}$$

1. Detector Output Proportional to Input Power

$$\text{Power into load } P_L = \frac{V^2 n_1^2 n_2^2 R_0}{(R_0 n_1^2 + r + R_0 n_2^2)^2}$$

$$\text{Max. power generator can deliver } P_0 = \frac{(Vn_1)^2}{4(n_1^2 R_0)} \tag{19}$$

$$\Delta P_L = \frac{\partial P_L}{\partial r}\Delta r = \frac{2V^2 n_1^2 n_1^2 R_0}{(R_0 n_1^2 + r + R_0 n_2^2)^3}\Delta r$$

In the case of the transmission cavity we have two coupling coefficients whose optimum value we have to determine.

$$\frac{\partial(\Delta P_L)}{\partial(n_1^2 R_0)} = \frac{\partial(\Delta P_L)}{\partial(n_2^2 R_0)} = 0$$
$$\therefore n_1^2 R_0 = n_2^2 R_0 = r \tag{20}$$

which means that the input and output coupling should be identical. Relation 20 looks superficially like a matching condition. However, it should be noted that the input impedance to the cavity contains besides the cavity impedance the load impedance. Hence, the VSWR is

$$\frac{R_0 n^2 + r}{R_0 n^2}$$

which represents an undercoupled case. One never can overcouple a transmission cavity with equal input and output couplings. Putting condition (20) into (19) we get:

$$\frac{\Delta P_L}{P_0} = -\frac{8}{27}\frac{\Delta r}{r} = -\frac{8}{27}\frac{\Delta Q_0}{Q_0} = -\left(\frac{8}{27}\right) 4\pi\chi'' \eta Q_0 \tag{21}$$

2. Detector Output Proportional to Input Voltage

The voltage across the load

$$V_L = \frac{V n_1 n_2 R_0}{R_0 n_1^2 + r + R_0 n_2^2}$$

Again for max. sensitivity both couplings should be the same

$$\Delta V_L = \frac{\partial V_L}{\partial r}\Delta r = -V\left[\frac{n_2^2 R_0}{(r + 2R_0 n_2^2)^2}\right]\Delta r \tag{22}$$

$$\frac{\partial V_L}{\partial(n_2^2 R_0)} = 0 \qquad \therefore R_0 n^2 = \frac{r}{2} \tag{23}$$

$$\therefore \frac{\Delta V_L}{V} = -\frac{1}{8}\frac{\Delta r}{r} = -\frac{1}{8}\frac{\Delta Q_0}{Q_0} = -\frac{1}{8} 4\pi\chi'' \eta Q_0 \tag{24}$$

Fig. 4 is a plot of (12), (15), (19), and (22). It should be noted that the sensitivities of the reflection cavity are normalized to the input of the magic T (in Fig. 1) and not to the input of the cavity as in the transmission cases. This results in a 3-db decrease in output and causes the power sensitivity of the transmission cavity to look relatively higher. However this is somewhat arbitrary since a balanced transmission type scheme would also require a magic T with an accompanying reduction in usable power.

All the previous sensitivity expressions are proportional to χ''. For an unsaturated condition it may be replaced by χ' whenever the output is sensitive to phase changes in the cavity.[1]

It should be noted that we maximized the output from the detector. This will result in a maximum signal to noise ratio if the noise is a constant independent of the microwave power. This, however, is in general not the case and in the next section we will investigate the signal to noise ratio taking into account its dependence on the RF power.

V. MINIMUM DETECTABLE SIGNAL UNDER IDEAL CONDITIONS

The minimum signal is ultimately determined by the random thermal agitation. Due to this cause the power fluctuates by an amount $kT\Delta\nu$, where k is Boltzmann's constant, T the absolute temperature and $\Delta\nu$ the bandwidth. The minimum detectable microwave power will be then of the order of $kT\Delta\nu$. This is the problem one faces when designing sensitive microwave receivers. However, our problem is of a different nature. We want to detect a small change in the power level of a relatively large

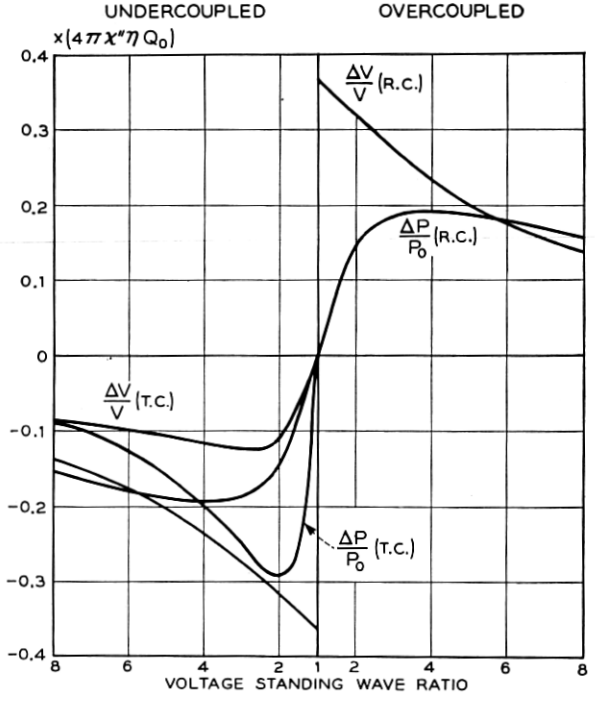

Fig. 4 — Output versus V.S.W.R. for reflection and transmission cavity.

microwave signal. This change in power level will have to be considerably larger than $kT\Delta\nu$ before it can be detected.[3] The physical reason for this is that the fluctuating fields associated with the noise power combine with the microwave fields to produce power fluctuations much larger than $kT\Delta\nu$. It is more straightforward to compare noise voltages rather than powers, especially since the power changes are not necessarily a constant of the system. In Fig. 1 for instance, the power change in arm 4 is

$$\Delta P_4 = \frac{(\Delta V)(V_4)}{R_0}$$

whereas the power change in arm 2 (for the same voltage change) is

$$\Delta P_2 = \frac{(\Delta V)(V_2)}{R_0}$$

It also shows that one wants to maximize the change in output voltage as was done in Section IV.

The open terminal RMS noise voltage of a system with an internal impedance R_0 is given by

$$V_{\text{RMS}} = \sqrt{4R_0kT\Delta\nu}$$

If we terminate this system with a noiseless resistor R_0, the voltage across it will be $\sqrt{R_0kT\Delta\nu}$. However, the terminating resistor is also at temperature T, so that the total RMS voltage across it will be $\sqrt{2}\sqrt{R_0kT\Delta\nu}$.

Comparing this RMS noise voltage with the signal voltage obtained in (16), we get for the reflection cavity*

$$\Delta V = V\sqrt{2}\pi\chi''\eta Q_0 = \sqrt{2}\sqrt{R_0kT\Delta\nu} \tag{25}$$

$$\therefore \chi_{\text{MIN}}'' = \frac{1}{Q_0\eta\pi}\left(\frac{kT\Delta\nu}{2P_0}\right)^{\frac{1}{2}} \tag{26}$$

As an example let us consider the following typical value for a 3-cm setup. $Q_0 = 5 \times 10^3$, $\Delta\nu = 0.1$ cps, $P_0 = 10^{-2}$ Watts

$$\eta = \frac{V_s}{V_c}\frac{4}{1+\left(\frac{d}{a}\right)^2} \simeq \frac{4V_s}{10\text{ cm}^3}.$$

For this case

$$(\chi_{\text{min}}'')(V_s) = \simeq 2 \times 10^{-14}$$

* In most cases the behaviour of the transmission and reflection cavity is similar, so that they will not be treated separately.

This corresponds for an unsaturated Lorentz line[1] to a static susceptibility $\chi_0 = \sqrt{3}\chi''(\Delta\omega/\omega)$, where $\Delta\omega$ is the line width between inflection points. For the free radical diphenyl picryl hydrazyl having a 2 oersted line width this expression at room temperature gives for the min. number of spins 10^{10}. A plot of the minimum RF susceptibility and minimum number of electrons versus microwave power is shown in Fig. 5.

VI. SIGNAL-TO-NOISE IN PRACTICAL SYSTEMS

A. General Considerations

1. Why Field Modulation?

From a design point of view it is instructive to consider the minimum fractional voltage change corresponding to the above $\chi_{\min}''V_s$ of 2×10^{-14}. This turns out to be, see (16),

$$\frac{\Delta V_{\min}}{V} \simeq 2 \times 10^{-10}.$$

From this figure one may safely conclude that it is not feasible to use any system in which the microwave carrier level reflected from the cavity has to be kept constant to this accuracy. Such systems would include straight detection, the dc being bucked out and amplified or systems employing amplitude modulation of the carrier. (Although

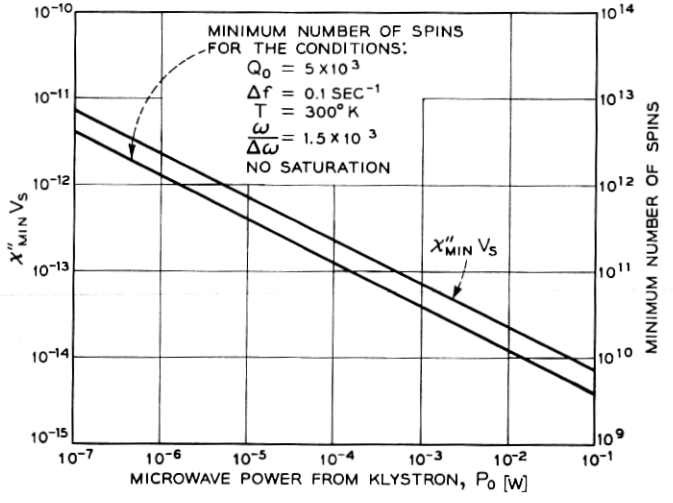

Fig. 5 — Minimum RF susceptibility and number of electrons which should be observable under thermal noise limitations. The conditions for the minimum number of spins correspond closely to those under which the experimental set-ups were tested.

the latter system may be improved by microwave bucking, it still remains very much inferior to the field modulation system to be described presently.) A system commonly used in which the requirements on the constancy of the microwave level is less stringent, makes use of a small external magnetic field modulation of angular frequency ω_M superimposed on the slowly varying dc magnetic field. Thus in the absence of a resonance line the output is zero except for some small Fourier components of the random fluctuations at the frequency ω_M. If the amplitude of the field modulation ΔH_M is small in comparison to the line width ΔH this method will sweep out the derivative of the line, i.e., the signal will not be proportional to χ'' as previously assumed but to $d\chi''/dH$ (ΔH_M). In order to preserve the line shape one should sweep only over a fraction of the line width. The sensitivity will thereby be reduced by roughly the same fraction. It should be noted, however, that even if one overmodulates the line (in order to increase the sensitivity) the resonance condition (i.e., place of zero signal, corresponding to new slope in the absorption) will not shift for a symmetrical line and the correct g-value may be obtained. Also from the knowledge of the amplitude of the modulating field the increase in line width may be corrected for. For those reasons we will not be concerned with the reduction in sensitivity due to this field modulation scheme.

2. Choice of Frequency

Referring to (26)

$$\chi_{\min} \propto \left(\frac{V_c}{V_s}\right)\frac{1}{Q_0}\frac{1}{\sqrt{P_0}}$$

and the minimum total number of electrons $N_{\min}$.

$$N_{\min} \propto \chi_0 V_s \propto \left(\frac{V_c}{Q_0}\right)\left(\frac{\Delta\omega}{\omega}\right)\frac{1}{\sqrt{P_0}} \tag{27}$$

Assuming that we are dealing with the same type of cavity mode at different frequencies, the same power, and that the line width $\Delta\omega$ is constant, we have $V_c \propto \frac{1}{\omega^3}$, $\quad Q_0 \propto \frac{1}{\omega^{\frac{1}{2}}}$

$$\therefore N_{\min} \propto \frac{1}{\omega^{7/2}} \tag{28}$$

Equation 28 shows that in order to see the smallest number of spins we want to go to as high as frequency as possible. The upper limit is given by the availability of components in the millimeter region, by the difficulty of handling them and by the maximum available power. The most commonly used setups operate at a wavelength of 1 cm and 3 cm.

The latter was used in the experimental part of this paper. From (28) we see that with a 1 cm setup the number of observable electrons should be approximately 40 times less than with a 3-cm setup. However, in most practical cases one is not limited by the amount of available sample, since one usually can increase the sample size at longer wavelengths. Therefore a better criterion is the minimum number of electrons per unit volume

$$\frac{N_{\min}}{V_s} \propto \left(\frac{V_c}{V_s}\right) \frac{1}{Q_0} \left(\frac{\Delta\omega}{\omega}\right) \tag{29}$$

Keeping now the filling factor V_c/V_s constant we see that the sensitivity of a 3 cm setup as defined in (29) is only $\sqrt{3}$ worse than of a 1 cm setup. In addition the power outputs of 3-cm klystrons are usually sufficiently higher than those of 1-cm klystron to overcome even the $\sqrt{3}$ advantage. If RF saturation comes in, the power argument is not valid, but one has to consider the RF magnetic field H_1 inside the cavity which for a given power and Q_0 is prop. to ω. Thus at the higher frequencies (1 cm) saturation effects become more pronounced reducing again the advantage of a 1-cm over a 3-cm setup. In deciding the choice of the frequency in special cases (e.g., when $\Delta\omega$ is a function of the magnetic field, or the sample is larger than a skin depth) (29) should be used.

There are, of course, considerations, other than those of max. sensitivity, which have to be taken into account. For example one would always like to satisfy the condition $\Delta\omega/\omega \ll 1$ which favors higher frequencies. On the other hand, for very narrow lines (say less than 0.1 oersteds) fractional field instabilities and inhomogeneities will favor low magnetic fields, i.e., lower frequencies. One also might encounter samples which exhibit an excessive loss in a given frequency band which therefore has to be avoided.

3. Optimum Amount of Sample to be Used

The output voltage ΔV is proportional to the sample volume and the unloaded Q_0 of the cavity, see (26). If the sample is lossy an increase in its size will reduce the Q and therefore reduce the signal. We may roughly distinguish two limiting cases. In one case the losses are proportional to E^2 (e.g., high resistivity samples having dielectric losses), in the other case they are proportional to H_1^2 (e.g., low resistivity samples in which the losses are due to surface currents).

a. Losses Proportional to E^2

The paramagnetic sample is placed in the region of max. RF magnetic field for instance at the end plate of a rectangular cavity resonating in

the TE_{10} mode. The sample extends a distance x into the cavity, x being assumed to be small in comparison to the wavelength so that H_1 does not vary appreciably over the sample. The additional losses due to the sample will then be proportional to

$$A \int_0^x E_0^2 \sin^2 \left(\frac{2\pi x}{\lambda}\right) dx \sim Cx^3$$

whereas the volume of the sample is proportional to x. The observed voltage change ΔV is then given by

$$\Delta V \propto Q_0' V_s \propto \left(\frac{1}{\frac{1}{Q_0} + Cx^3}\right)(x)$$

where Q_0 is the Q of the cavity without sample, and Q_0' the total Q of both cavity and sample. Maximizing the voltage change ΔV we get

$$\frac{\partial(\Delta V)}{\partial x} = 0 \qquad \therefore Cx^3 = \frac{1}{2Q_0} \tag{30}$$

$$\therefore Q_0' = \tfrac{2}{3} Q_0$$

Equation (30) tells us that we should load the cavity with the sample until the Q_0 is reduced to $\frac{2}{3}$ of its original value. It should be pointed out that we optimized the signal and not the more important quantity, the signal-to-noise ratio. Therefore the analysis is only valid as long as the noise is not a function of Q_0, (see Section VIB) and that we do not saturate the sample (see Section VIII). If either condition does not hold the amount of sample to be put in should exceed the above calculated value.

b. Losses Proportional to H_1^2

The losses do not vary along the sample so that we may write

$$\Delta V \propto Q_0' V_s \propto \left(\frac{1}{\frac{1}{Q_0} + Cx}\right)(x)$$

which clearly has no maximum for x. One should therefore put as big a sample into the cavity as possible (compatible with the assumption that if it be small in comparison to a wavelength), the same result as if one had no losses at all.

B. Noise Due to Frequency Instabilities

Before considering the signal-to-noise ratio for specific systems we will investigate a noise source which is common to all of them. It arises

from the random frequency variations of the microwave source or from the random variations of the resonant frequency of the cavity (e.g., rising helium bubbles at 4°K or just any microphonics).

From the equivalent circuit of a reflection cavity (see Fig. 2) we can write for the voltage standing wave ratio

$$\text{VSWR} = \frac{Z_{in}}{R_0 n^2} = \frac{r}{R_0 n^2} + \frac{j}{R_0 n^2}\left(\omega L - \frac{1}{\omega C}\right)$$

$$= \frac{r}{R_0 n^2}\left[1 + jQ_0\left(\frac{2\Delta\omega}{\omega}\right)\right] = \frac{r}{R_0 n^2}\left[1 + j\delta\right]$$

where $\delta = Q_0(2\Delta\omega/\omega)$ and $\Delta\omega$ is the frequency deviation from the resonant frequency of the cavity. The reflection coefficient Γ is then given by:

$$\Gamma = \frac{\frac{r}{R_0 n^2}(1 + j\delta) - 1}{\frac{r}{R_0 n^2}(1 + j\delta) + 1} = \Gamma_0 + 2\frac{\frac{R_0 n^2}{r}\delta^2}{\left(\frac{R_0 n^2}{r} + 1\right)^3} + 2j\frac{\frac{R_0 n^2}{r}\delta}{\left(\frac{R_0 n^2}{r} + 1\right)^2}$$

where Γ_0 is the reflection coefficient at the resonant frequency of the cavity. The other two terms giving the changes in Γ for a given frequency deviation $\Delta\omega$. The changes of $\Delta\omega$ (or $\Delta\Gamma$) having ac components near the modulation frequency will thus represent noise terms which will pass together with the signal through the detection system. The slide screw tuner (see Fig. 1) which is used to buck out part of the microwave power will introduce an additional reflection coefficient $\Gamma_R + j\Gamma_R'$. Thus the total reflection coefficient will be given by

$$\Gamma = \Gamma_0 - \Gamma_R + 2\frac{\frac{R_0 n^2}{r}\delta^2}{\left(\frac{R_0 n^2}{r} + 1\right)^3} - j\Gamma_R' + j2\frac{\frac{R_0 n^2}{r}\delta}{\left(\frac{R_0 n^2}{r} + 1\right)^2} \tag{31}$$

We are interested only in the magnitude of V (i.e., $|\Gamma|$) reaching the detector. Tuning to the dispersion mode (χ') the slide screw tuner is adjusted such that $\Gamma_R' \gg \Gamma_0 - \Gamma_R$. Under these conditions the output noise voltage will be given by

$$\left(\frac{\Delta V_N}{V}\right)_{\chi'} \simeq 2\frac{\frac{R_0 n^2}{r}\delta}{\left(\frac{R_0 n^2}{r} + 1\right)^2} \tag{32}$$

Tuning to the absorption (χ''), the condition $\Gamma_0 - \Gamma_R \gg \Gamma_R$ will be

satisfied and (31) becomes

$$\left(\frac{\Delta V_N}{V}\right)_{\chi''} \simeq 2\frac{\left(\frac{R_0n^2}{r}\right)\delta^2}{\left(\frac{R_0n^2}{r}+1\right)^3} + 2\frac{\left(\frac{R_0n^2}{r}\right)^2\delta^2}{\left(\frac{R_0n^2}{r}+1\right)^4(\Gamma_0-\Gamma_R)} \tag{33}$$

An inspection of (31), (32), and (33) shows that the noise voltage, enters as a first order effect in δ when tuned to χ'. This is not too surprising since a frequency effect is expected to affect predominantly the dispersion mode. When tuned to χ'' the effect becomes second order as long as $|\Gamma_0 - \Gamma_R|$ is large. Under those conditions the 2 terms in (33) are of comparable magnitude. We can easily see the origin of the second term. It arises from the first order out-of-phase component of the noise voltage. Being, however, sensitive only to in-phase components it will be reduced to a second order effect—as long as $|\Gamma_0 - \Gamma_R|$ is large, i.e., as long as we have a carrier which makes us insensitive to out-of-phase components.* When $\Gamma_0 - \Gamma_R$ goes to zero (33) ceases to hold and the noise voltage will be given by (32).

There are two important conclusions to be drawn from (33).

We want to keep $\Gamma_0 - \Gamma_R$ as large as possible. Therefore in schemes (like the superheterodyne see section VI E) where this is not feasible, special care has to be taken to eliminate this noise source.

From (15) we find that the desired signal is proportional to

$$\frac{R_0n^2}{r}\Big/\left(\frac{R_0n^2}{r}+1\right)^2$$

Comparing this expression with (33) we see that the signal-to-noise ratio may be improved by increasing R_0n^2/r, i.e., overcoupling the cavity until this noise source does not contribute any more. A comparison of (15) with (32) shows that overcoupling will not improve the signal-to-noise ratio when tuned to χ'. In this connection it should be pointed out that only those frequency stabilization schemes can alleviate the problem of frequency instabilities whose response time is at least of the order to the inverse modulation frequency since the troublesome noise components are at this frequency. Some stabilization schemes make use of the cavity into which the sample is placed as the stabilizing element. Although this system may be excellent for the observation of χ'' (it is the only one which can compensate for cavity microphonic), it fails in the case of χ'. The reason is that χ' makes itself observable essentially by a frequency shift which in this scheme would be compensated for.

* For a similar reason one cannot avoid an admixture of dispersion to an absorption signal, when investigating a saturated sample in which $\chi'_{max} \gg \chi''_{max}$.

C. Noise Due to Cavity Vibrations

A noise source which can be very troublesome at high modulation fields arises from the currents induced in the walls of the cavity from the modulating field. The interaction of these currents with the dc magnetic field causes mechanical vibrations of the cavity walls. This produces a signal when tuned to the dispersion, but to first order should give no signal when one is tuned to the cavity and sensitive to the absorption. However, any detuning will result in a signal, which, having the right frequency will pass through the narrow band amplifier and lock-in detector. Since this signal is proportional to the magnetic field, it will result in a background signal whose amplitude will vary as the magnetic field is being swept and thus causing a continuous shift in the base line. In a rectangular cavity this effect can be greatly reduced by a proper orientation of the cavity with respect to the dc magnetic field. This is due to the fact that by squeezing the broad face of a rectangular cavity (TE_{10} mode) the frequency decreases, whereas by squeezing the narrow walls of the cavity the frequency increases. Thus in a proper orientation the two effects cancel each other out. We found another way of greatly reducing the effect by using a glass cavity having a silver coating* thick in comparison to a microwave skin depth but small in comparison to the modulation frequency skin depth, thereby decreasing the eddy currents without impairing the mechanical strength of the cavity.

D. Klystron Noise

There is very little data available on presently used klystrons. The data quoted by Hamilton, et al[4] are on a 723A klystron. With an IF of 30 mc, bandwidth of 2.5-mc microwave output of 50 mw they obtained a noise power of 5×10^{-12} watts. Expressing their results in terms of a noise figure N_k such that the noise power output in the two side bands P_k is given by

$$P_k = 2N_k(kT\Delta\nu) \qquad \therefore N_k = \frac{1}{2}\left(\frac{P_k}{P_0}\right)\frac{P_0}{kT\Delta\nu} = sP_0 \qquad (34)$$

Substituting their numerical values one obtains for $s = 5000$ Watt^{-1}. The values for s that we obtained with a 60 mc IF are:

Higher mode of V-153 klystron	$s \simeq 1{,}000$ Watt^{-1}
Lower mode of V-153 klystron	$s \simeq 3{,}000$ Watt^{-1}
Higher mode of X-13 klystron	$s \simeq 200$ Watt^{-1}
Lower mode of X-13 klystron	$s \simeq 400$ Watt^{-1}

* We are indebted to A. V. Hollenberg and V. J. DeLucca for the making of the glass cavities and to A. W. Treptow for the excellent silver coatings.

The method used to determine the above noise figures is similar to the one described in Reference 4. The figures are expected to be several times larger when a 30 mc IF is used. (A factor of 2 is quoted by Hamilton, et al.[4]) It is also worth noting that the relative noise power decreases on going to higher modes.

E. Signal-to-Noise Ratio for Specific Systems

In this section we will analyze specific systems under varying conditions. The reason why we do not present the analysis of one "The Best" system is that sometimes a compromise between complexity and sensitivity has to be reached and also because some systems may be superior at high power whereas others at low powers.

The expression for the noise power P_N at the output of the microwave detector (X-tal or bolometer) is[5]

$$P_N = (GN_K + F_{\text{AMPL}} + t - 1)(kT\Delta\nu) \tag{35}$$

where:

G = conversion gain of the detector (generally smaller than one. A quantity often used instead of G is the conversion loss $L = 1/G$).

N_K = noise figure at the input of the detector. Usually due to random amplitude or frequency fluctuations of the microwave source or the microwave components (see Section VID).

F_{AMPL} = noise figure of the amplifier

t = noise temperature of the detector

Comparing the equivalent voltage fluctuations of this noise power with the signal voltage as derived in (26), we get for the minimum detectable χ''

$$\chi_{\text{min}}'' = \frac{1}{Q_0\eta\pi}\left[\frac{(GN_k + F_{\text{AMP}} + t - 1)kT\Delta\nu}{2GP_0}\right]^{\frac{1}{2}} \tag{36}$$

The above relation should apply to all systems. The problem then reduces to the determination of G, N_k, F_{AMP}, and t for the particular detection scheme. A difficulty arises from the fact that not only are those quantities a function of the RF power and modulation frequency but in the case of detectors vary from unit to unit. It is probably for this reason that the values quoted in the literature are sparse and are not in agreement with each other. The values used in this analysis for the X-band barretters (821) and crystals (1N23C) were obtained by us. Values for K-band crystals can be found in References 6 and 7. It should also be borne in mind that the values are time dependent and

will have to be modified as the "art" of detector manufacturing improves. Also new systems might come into prominence in the near future. An example would be the use of low noise travelling wave tubes preceding the detector or even low noise solid state masers.

1. Barretter (bolometer) detection.

The resistance of a barretter is given by the relation[2]

$$R = R_0 + kP^n \tag{37}$$

For practical purposes n may be taken as unity. The instantaneous power input to the barretter for a modulated microwave is given by

$$P = \frac{1}{R}\left[V_0 \sin \Omega t \left(1 + \frac{\Delta V}{V_0} \sin \omega t\right) + V_{dc}\right]^2 \tag{38}$$

where V_0 is the amplitude of the microwaves, ΔV the change of the amplitude due to the absorption given by (16), Ω the microwave frequency, ω the field modulation frequency, and V_{dc} the bias on the barretter. Expanding (38) and assuming that $\Delta V/V_0 \ll 1$ we get, after throwing out the high frequency terms,

$$R = R_0 + k\left(P_{RF} + P_{dc} + \frac{V_0 \Delta V}{R} \sin \omega t\right) \tag{39}$$

where P_{RF} is the power in the unmodulated carrier reaching the barretter. It is of course smaller than P_0 the microwave power from the klystron because of the power splitting in the magic T and the reflection from the cavity. Taking a reflection coefficient $\Gamma \simeq 0.5$ (see Section IVA), $P_{RF}/P_0 \simeq 0.1$. The desired voltage fluctuation associated with the resistance change is: $\delta V = I_0 \Delta R$, where

$$\Delta R = \frac{dR}{dP}\Delta P = \frac{dR}{dP}(\Delta P_{RF} + I_0^2 \Delta R), = \frac{dR}{dP}\left[\frac{1}{1 - I_0^2 \dfrac{dR}{dP}}\right]\Delta P_{RF}$$

$$\therefore \delta V \simeq I_0 k \frac{V_0 \Delta V}{(1 - I_0^2 k)} \sin \omega t \tag{40}$$

I_0 is the current bias on the barretter which we want to keep constant for a maximum voltage change δV.

The power gain of this device G is given by

$$G = \frac{\text{Signal Power from Barretter}}{\text{Power in the Sidebands}} = \frac{\delta V^2}{2R} \Big/ \frac{\Delta V^2}{4R} = 4 \frac{I_0^2 k^2 P_{RF}}{R(1 - I_0^2 k)}$$

$$= 4k^2 \frac{P_{dc} P_{RF}}{R^2(1 - I_0^2 k)} \tag{41}$$

The noise figure of the audio amplifier following the detector is given in general by:

$$F_{\text{AMP}} = \frac{R_{\text{equ}} + R_G}{R_G} \tag{42}$$

where R_G is the generator input resistance in this case the barretter resistance and R_{equ} is an equivalent noise resistor in series with the generators. The best input tube that we found was the General Electric GL 6072 triode* for which we measured an R_{equ} at 100 c.p.s. of $\sim 10^5\ \Omega$. (This is due to flicker noise of the tube and has a $1/f$ dependence.) If we were to connect the barretter, having a resistance of $\sim 200\ \Omega$ straight to the grid of the input tube we would get a noise figure of ~ 500. However, by using a step-up transformer with a turns ratio $n > \frac{R_{\text{equ}}}{R_B}$ the noise figure of the amplifier can be reduced to nearly unity. We will assume in the following analysis that this has been done.

The noise temperature of the barretter t_B was thought to be approximately 2 since it is merely a platinum wire operating at an elevated temperature. To our surprise the measured value turned out to vary for different units between 4 and 40.† The noise figure was measured on about 20 different units obtained from 4 different manufacturers (P.R.D.; F.X.R. Narda, Sperry). The reason for this noise is not entirely clear at present. A possible explanation is the non-uniform heating of the wire which could set up air currents. They in turn can cool the wire in a random fashion giving rise to an additional noise component. An improvement of the noise figure was noted upon evacuating the barretter. The noise figure of a unit which was initially 10, dropped to the expected value of 2 after evacuation. However, it should be pointed out that this cannot be taken as a definite proof for the "air current theory" since the characteristics of the barretter changed markedly after evacuation. The sensitivity of the evacuated barretter went up from $5\Omega/mW$ to $200\Omega/mW$ which necessitated a reduction of the dc current from 8 to 1.5 mA. Also the response time went up by a factor of 20, so that the effectiveness of any noise mechanism with a $1/f$ spectrum would be greatly reduced. This approach however looks definitely promising in trying to design more sensitive and less noisy barretters. In the present work commercial unevacuated barretters were used, their noise temperature being taken as 4 in the following analysis. Under

* We are indebted to R. G. Shulman for bringing this tube to our attention.

† One unit which exhibited an extremely large noise figure of 1,000 was eliminated entirely. The solder point of the platinum wire was apparently defective.

those assumptions (36) becomes:

$$\chi''_{\text{MIN}} = \frac{1}{Q_0\eta\pi}\left(\frac{kT\Delta\nu}{P_0}\right)^{\frac{1}{2}}\left(\frac{4 + N_k G}{G}\right)^{\frac{1}{2}} \tag{43}$$

a. Straight detection

A block diagram of the microwave part of a simple barretter system is shown in Fig. 6. The attenuator serves the purpose of preventing power saturation of the sample or burn out of the bolometer at high powers. By means of the slide screw tuner and magic T arrangement one makes the system sensitive to either the real or imaginary part of the susceptibility.

The characteristics of a typical barretter (like the Sperry No. 821) are: $R = 250\ \Omega$; $k = 4.5\ \Omega/mW$; $P_{\text{MAX}} = 32\ mW$. We take the worst generator noise figure reported, i.e., $N_k = 5{,}000\ P_{\text{RF}}$ (see Section VID).

The ratio of the minimum susceptibility $\chi''_{\text{MIN-OBS}}$ that can be detected with this system to the minimum theoretical value if one were limited by thermal noise only becomes with the aid of (41) and (43)

$$\frac{\chi''_{\text{MIN-OBS}}}{\chi''_{\text{MIN-TH}}} = \left(\frac{4 + N_K G}{G}\right)^{\frac{1}{2}} = \left(\frac{1 + 5 \times 10^3 P_{RF} k^2 \dfrac{P_{RF}P_{\text{de}}}{R^2(1 - I_0{}^2 k)}}{k^2 \dfrac{P_{RF}P_{\text{de}}}{R^2(1 - I_0{}^2 k)}}\right)^{\frac{1}{2}} \tag{44}$$

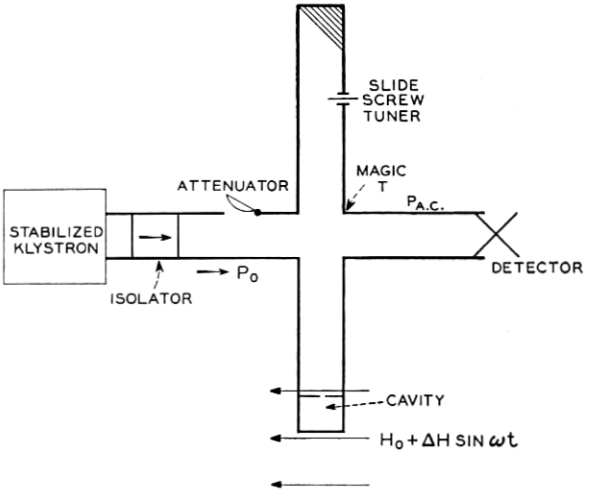

Fig. 6 — Essential microwave parts of a simple barretter or crystal set-up.

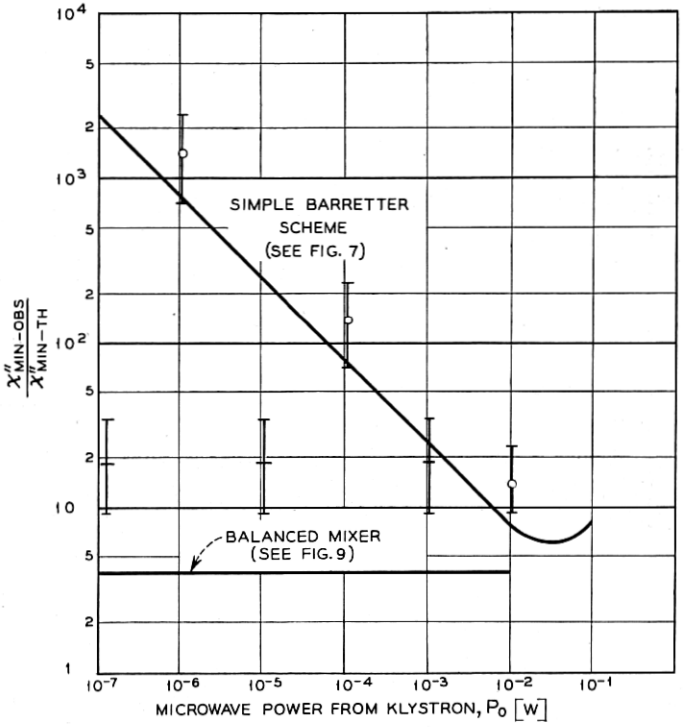

Fig. 7 — The ratio of the minimum detectable susceptibility to the minimum theoretical value versus microwave power for 2 different barretter schemes. Full lines correspond to the predicted sensitivity and dots indicate experimental values.

Equation (44) is plotted in Fig. 7. From this plot we see that the system is extremely poor at low powers (which is due to the low conversion gain of barretters) and also starts getting worse at high powers (due to the signal generator noise). The latter point is not of great importance since one can always buck down the microwave power by means of the slide screw tuner to the desired level. By using the evacuated barretter as mentioned earlier, the curve in Fig. 7 would be shifted to the left corresponding to the increased conversion gain.

b. Balanced mixer detection

An improved barretter scheme is shown in Fig. 8. It eliminates the poor conversion gain at low powers by employing a balanced mixer into which a large amount of microwave power P_2 can be fed from the same signal generator. Since the barretter noise should not be power

dependent (unlike in crystals) this procedure improves the conversion gain without increasing the noise. Since a balanced mixer is used the noise from the signal generator is also cancelled. A necessary precaution in this set-up is to include extra isolation between the second magic T and the mixer in order to prevent any microwave power from leaking through the balanced mixer into the cavity.

For this arrangement (44) becomes:

$$\frac{\chi''_{\text{MIN-OBS}}}{\chi''_{\text{MIN-TH}}} \sqrt{2} \sqrt{\frac{4}{G}} \tag{45}$$

The factor of $\sqrt{2}$ arises from the fact that we had to split the power P_0 in the first magic T. Since in this scheme we are at liberty to vary the input power to the barretter we want to maximize G with respect to P_2. For a fixed total power to the barretter given by its burn-out ratings (i.e., $P_2 + P_{dc}$ = constant) (41) is a maximum for $P_2 \simeq P_{dc} \simeq \frac{P_{MAX}}{2}$. Taking again the data for the No. 821 barretter we get for $G_{MAX} \simeq 0.5$ and for

$$\frac{\chi''_{\text{MIN-OBS}}}{\chi''_{\text{MIN-TH}}} \simeq 4 \tag{46}$$

Since the value of P_2 can be held constant irrespective of the power in the cavity, this ratio will be a constant (see Fig. 7).

It should be pointed out that in this system a wrong phasing of arm P_2 will result not only in a reduction of the signal, but also in an admixture of χ' and χ''. Therefore after changing the power by means of a

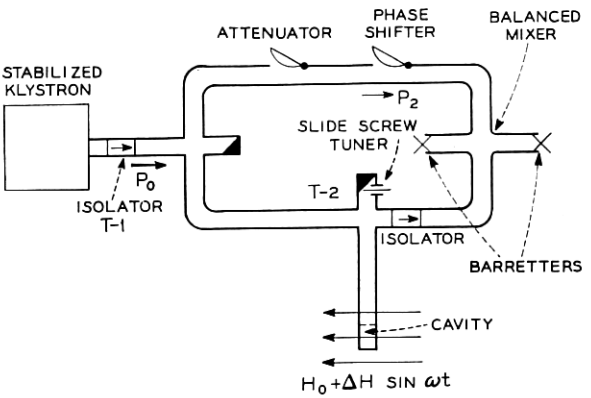

Fig. 8 — Barretter system with balanced mixer.

variable flap* attenuator (which also introduces a phase shift) or after changing the slide screw tuner the system has to be rephased again. This makes saturation measurements less convenient than in the superheterodyne system to be discussed in the next section. The obvious advantage of the homodyne detection scheme is that it requires only one microwave oscillator.

2. Crystal detection

A simple set-up is shown in Fig. 6. Although its microwave components are identical to the ones used in the barretter scheme, the analysis of this set-up is more complicated. The reason is that not only do crystal characteristics vary greatly from unit to unit but they cannot be described by one simple relation over the entire range of incident microwave power. One can roughly divide their characteristics into a square law region where the rectified current I is proportional to P_0 (holds for $P_0 < 10^{-5}$ Watts) and the linear region where I is proportional to $\sqrt{P_0}$. (holds for $P_0 > 10^{-4}$ Watts). The output noise of a crystal can be represented in general by the relation.[5, 8, 9]

$$P_N = \left(\frac{\alpha I_0^2}{f} + 1\right) kT\Delta\nu \dagger \tag{47}$$

where f is the frequency around which the bandwith $\Delta\nu$ is centered. This relation reduces for the square law region to:

$$P_N = \left(\frac{\beta P_{RF}^2}{f} + 1\right) kT\Delta\delta \tag{48}$$

and for the linear region to

$$P_N = \left(\frac{\gamma P_{RF}}{f} + 1\right) kT\Delta\nu \tag{49}$$

The average values of β we determined experimentally are:

$$\beta \simeq 5 \times 10^{14} \text{ Watt}^{-2} \text{ sec}^{-1} \quad \text{and}$$

$$\gamma \simeq 10^{11} \text{ Watt}^{-1} \text{ sec}^{-1}$$

The conversion gain G of the crystal can be represented by

$$G = SP_{RF} \tag{50}$$

in the square law region and by

$$G = \text{constant} = C \tag{51}$$

* The phase shift associated with the Hewlett-Packard X-382-A attenuator is quite small.

† Values of α for K-band crystals are quoted in References 6 and 7. They differ however from each other by approximately 3 orders of magnitude.

in the linear region. Values of S and C for the 1N23C were found to be $S \simeq 500$ Watt^{-1} and $C \simeq 0.3$.

a. Simple straight detection

If one does not make use of the bucking possibilities of the magic T (i.e., eliminate the slide screw turner in Fig. 6) one has the simplest possible set-up sensitive to χ''. Under those conditions the microwave power reaching the crystal will be identical to the reflected power from the cavity. Equation (36) becomes:

$$\frac{\chi''_{\text{MIN-OBS}}}{\chi''_{\text{MIN-TH}}} = \left(\frac{GN_k + F_{\text{AMP}} + t - 1}{G}\right)^{\frac{1}{2}} \tag{52}$$

With the aid of (48), (49), (50), and (51), this relation reduces for the 1N23C in the square law region to:

$$\frac{\chi''_{\text{MIN-OBS}}}{\chi''_{\text{MIN-TH}}} = \left(\frac{1 + 5 \times 10^9 P_0^2}{50 P_0}\right)^{\frac{1}{2}} \tag{53}$$

and for the linear region to:

$$\frac{\chi''_{\text{MIN-OBS}}}{\chi''_{\text{MIN-TH}}} = (3 \times 10^7 P_0)^{\frac{1}{2}} \tag{54}$$

A plot of (53) and (54) is shown in Fig. 9. As before the assumption was made that $P_{\text{RF}}/P_0 \simeq 0.1$ (see barretter case). The noise figure of the amplifier F_{AMP} was taken as unity which again can be closely approached by means of a step-up transformer. The field modulation frequency was assumed to be 1,000 c.p.sec., although (47) shows that from a point of view of noise one would like to go to as high a frequency as possible. However practical consideration such as power requirements for getting a given modulation field, pick-up problems, skin depth losses in the cavity wall usually set an upper limit. The modulation frequency may be also dictated at times by the relaxation times of the investigated sample.[10]

b. Straight detection with optimum microwave bucking

From Fig. 9, we see that the straight crystal detection scheme suffers at low powers because of the poor conversion gain of the crystal and at high powers because of excess crystal noise. This situation can be greatly improved by adding some microwave power to the crystal when the reflected power from the cavity is low (to be referred to as positive bucking) or subtracting some of the power in the other case (negative bucking). In this section we will find the improvement over the unbucked system and the amount of bucking required to effect it.

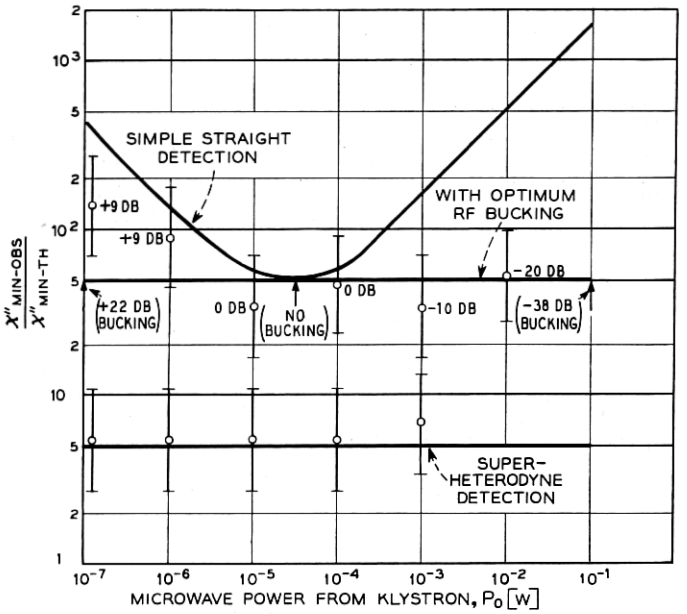

Fig. 9 — The ratio of the minimum observable susceptibility to the minimum theoretical value versus microwave power for different crystal detection schemes. Full lines correspond to the predicted sensitivity and dots indicate experimental values.

We define the bucking parameter B by the relation

$$P_x = BP_{RF} \tag{55}$$

Where P_{RF} is the microwave power at the crystal before and P_x after the bucking is applied. We further assume that after the bucking is applied the crystals will operate in the square low region. Combining (49), (50), and (52) and neglecting the term GN_k which is small in comparison to the other term we get for the bucking scheme:

$$\frac{\chi''_{\text{MIN-OBS}}}{\chi''_{\text{MIN-TH}}} = \left(\frac{F_{\text{AMP}} + \frac{\beta B^2 P_{RF}^2}{f}}{SBP_{RF}} \right)^{\frac{1}{2}} \tag{56}$$

In order to find the optimum bucking parameter, we set

$$\frac{d}{dB}\left(\frac{\chi''_{\text{MIN-OBS}}}{\chi''_{\text{MIN-TH}}} \right) = 0 \text{ which results in}$$

$$\left(B = \frac{F_{\text{AMP}} f}{\beta P_{RF}^2} \right)^{\frac{1}{2}} \tag{57}$$

Putting in the numerical values for the 1N23C as quoted previously we get that $B = 1.4 \times 10^{-6}/P_{RF}$. Equation (56) becomes with the optimum bucking parameter

$$\frac{\chi''_{\text{MIN-OBS}}}{\chi''_{\text{MIN-TH}}} = \left[\frac{2F_{\text{AMP}}}{S\left(\frac{F_{\text{AMP}}f}{\beta}\right)^{\frac{1}{2}}}\right] \tag{58}$$

For the case under discussion this ratio turns out to be $\simeq 50$ independent of P_0. Fig. 9 shows a plot of (58). The values in parenthesis indicate the degree of bucking necessary to accomplish this ratio as determined from (57). It should be noted that the negative bucking can be easily accomplished by means of the slide screw tuner in the magic T arm (see Fig. 6) whereas for large positive buckings a scheme like in Fig. 8 has to be used. (Some positive bucking can of course be also accomplished by means of the slide screw tuner).

c. The superheterodyne scheme

The RF bucking system just described bears a certain resemblance to the balanced mixer barretter scheme. In both cases additional microwave power was added to the detector in order to increase the conversion gain. However in the crystal scheme this resulted in an increase in noise power whereas this should not be the case with barretters. The question arises whether a decent conversion gain in crystals has to be always accompanied by a large noise power. An inspection of (49) shows that around frequencies of tens of megacycles* or higher the noise output of the crystal becomes negligible. As pointed out earlier such high magnetic field modulation frequencies are not feasible. However in a superheterodyne system the crystal outputs will be at an intermediate frequency of 30 or 60 mc. This will make the flicker noise components negligible even at high powers where the conversion gain is good. The conventional way to obtain the intermediate frequency is to beat the reflected signal from the cavity with a local oscillator (see Fig. 10) which is removed from the signal generator by the I.F. frequency. In order to eliminate the noise from the local oscillator a balanced mixer should be employed. The ratio

$$\left(\frac{\chi''_{\text{MIN-OBS}}}{\chi''_{\text{MIN-TH}}}\right) \text{ becomes then from equ. 52 } \left(\frac{F_{IF} + t - 1}{G}\right)^{\frac{1}{2}} \tag{59}$$

The expression in the brackets is called in radar work[11] the overall

* It was shown by G. R. Nicoll[9] that this equation holds up to this frequency range.

noise figure of the receiver F. We found that a noise figure of about 11–14 db is easily attainable with commercial I.F. amplifiers and balanced mixer. This would give us a ratio of

$$\frac{\chi''_{\text{MIN-OBS}}}{\chi''_{\text{MIN-TH}}} \simeq 5$$

which is plotted together with the other crystal schemes in Fig. 9. Although this system does necessitate 2 stable microwave sources, it is not difficult to operate once they are set-up. This was not considered as a major disadvantage at least not at X-band. The phasing problem discussed in connection with the mixer barretter scheme of comparable sensitivity is eliminated. An additional small advantage is the ruggedness of crystals in comparison to barretters and the availability of good commercial balanced crystal mixers. There are other double frequency schemes which do not need 2 separate microwave signal generators. The other frequency may be obtained by amplitude or phase modulating one signal generator by an IF frequency. The side bands which are produced in this way are displaced by just the IF frequency and may be utilized instead of the second signal generator. Schemes of this sort look particularly promising for frequencies well above X-band in which case it might prove difficult to maintain the difference frequency of two separate microwave generators within the band width of the IF.

F. Experimental Determination of Sensitivity Limits

1. Preparation of samples

In order to get an experimental check on the previous analysis, samples with a known number of spins had to be prepared. Two sets of samples were made. One consisted of single $CuSO_4 \cdot 5H_2O$ crystals of varying sizes hermetically sealed between 2 sheets of polyethylene. The other set consisted of different amounts of diphenyl picryl hydrazyl* which were similarly sealed up. D.P.H. samples having less than 10^{17} spins were prepared by dissolving known amounts of the free radical in benzene and putting a drop of this solution on the polyethylene. After the benzene had evaporated, it was sealed up with another sheet of polyethylene. The g-values of $CuSO_4 \cdot 5H_2O$ and D.P.H. differ enough so that both samples can be conveniently run simultaneously. This was done in order to check the self consistency of the two sets of samples. The measured integrated susceptibility of all the D.P.H. samples

* We are indebted to A. N. Holden for supplying us with this material.

with more than 10^{16} spins agreed within a few percent with the calculated value. The calculated value being based on the known amount of D.P.H. and the measured value being referred to the known amount of $CuSO_4 \cdot 5H_2O$. D.P.H. samples with less than 10^{16} spins had all a smaller number of effective spins than calculated. The discrepancy was more pronounced the smaller the sample. There was also evidence that the smaller D.P.H. samples deteriorated with time. As a typical example we quote a sample which started out as 10^{15} effective spins and was reduced after 4 weeks to 4×10^{14} effective spins and another one which initially had 10^{14} spins, deteriorated in the same time interval to 10^{13} spins. Since only the smaller samples were noticeably affected, this deterioration seems to be associated with a surface reaction. It was also observed that the line width between inflection points of the D.P.H. samples with less than 10^{15} spins increased from 1.8 oersteds to 2.7 oersteds. This broadening probably arises from a reduction in the exchange narrowing mechanism due to the spreading out of the sample.

2. Comparison of experimental results with theory

In checking the sensitivity of the equipment D.P.H. samples were used and the signal to noise was estimated from the recorded output. The experimental points thus obtained are shown in Fig. 7 and Fig. 9. We believe that the results are significant to within a factor of 2, the main error arising from the estimate of the RMS noise. The band width of the lock-in detector was $\Delta\nu = 0.03$ sec^{-1}, $Q_0 = 4{,}000$, and the field modulation used was 3 oersteds p.t.p., 100 c.p.sec. for the barretter schemes and 1,000 c.p.sec. for the crystal schemes. This large modulation field somewhat distorts the line, but, as mentioned earlier was done in order to get the full signal. The D.P.H. samples were calibrated against $CuSO_4 \cdot 5H_2O$ before each run. Even so it was not felt safe to use samples which had less than 10^{13} spins.

Referring to Fig. 8 we see that for the straight barretter detector the experimental points agree fairly well with the predicted value, but in the balanced mixer scheme fall short by about a factor of 4. A possible explanation of this discrepancy is that the barretters were not completely matched in which case the noise from the local oscillator would not be compensated for.

Fig. 9 shows the experimental points for the crystal schemes. For powers between 10^{-7} W and 10^{-5} W the system used fell between the simple straight detection scheme and the one utilizing optimum RF bucking. The reason is that it was very easy to obtain a certain amount of positive bucking (+9 db) by merely adjusting one arm of the magic T.

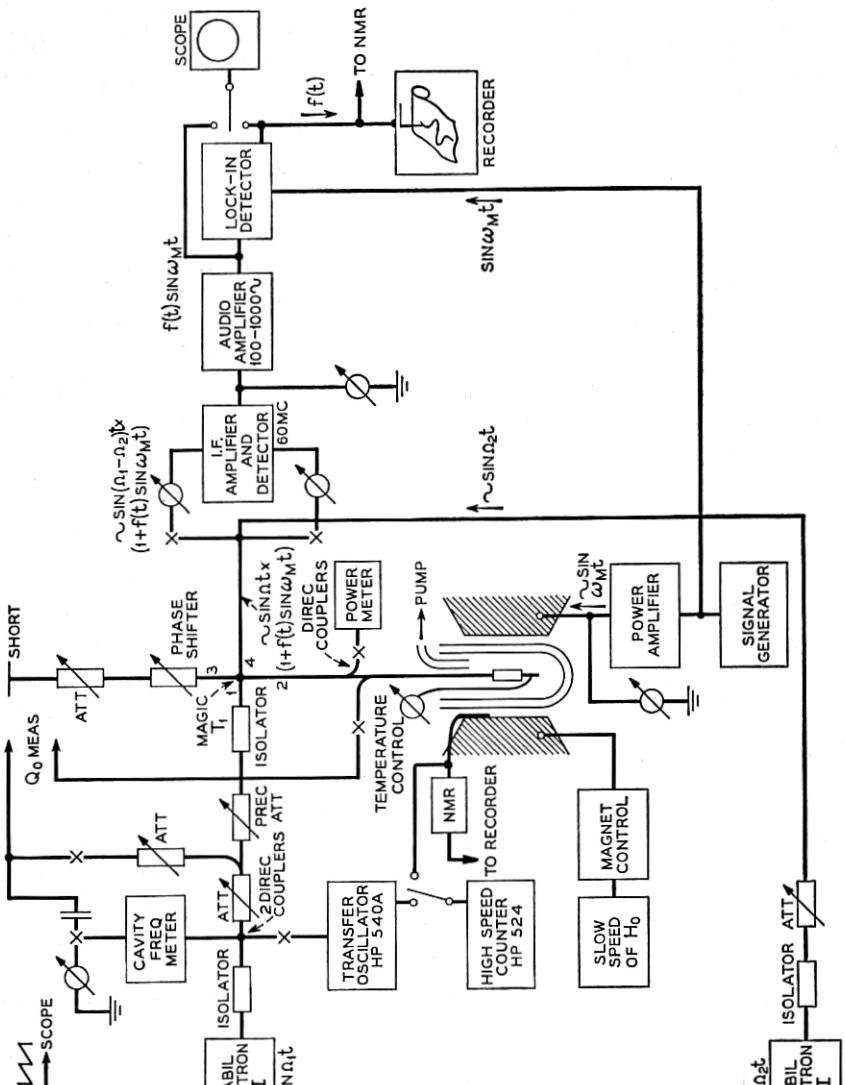

Fig. 10 — Block diagram of a superheterodyne paramagnetic resonance spectrometer.

It would however have been a great deal more difficult to obtain the entire bucking of +22 db at 10^{-7} W since a set-up like in Fig. 8 would have to be used. Thus for the sake of simplicity the extra factor in signal to noise of 2 or 3 was abandoned. The amount of negative bucking at the higher powers will be limited by the stability of the bridge. A practical limit of (40–50) db was characteristic of our set-up. We see from Fig. 9 that the agreement between the experimentally determined sensitivity and the theoretically predicted sensitivity is satisfactory.

The experimental results on the superheterodyne scheme agrees again very well with the predicted values up to a power level of 10^{-3} W. (This corresponds to less than 10^{12} spins in D.P.H.) Above this level T_1 (see fig. 10) has to be balanced to better than 40 db to keep the IF carrier amplitude within the required value. Instabilities in the bridge due to mechanical vibrations and thermal drifts start to contribute to the noise. Thus at high power levels the superhet scheme starts to loose some of its advantages unless special precautions are being taken to eliminate the above mentioned noise factors. A great deal in this direction could probably be accomplished by shock-mounting the microwave components and better temperature stability for slow drifts. Since we were mainly interested in powers below 1 mW, our efforts were limited to controlling the temperature of the room to $\pm 1°C$.

Since the superhet scheme was found to be the most sensitive one, it might be worthwhile to discuss it in more detail. A block diagram of the set up is shown in Fig. 10.

The signal generator feeds into the magic T, where its power is split between arm 2 and 3. Arm 2 has the reflection cavity with the sample, the reflected voltage being bucked out with the aid of arm 3. For this purpose arm 3 has a phase shifter and attenuator, an arrangement which was found to be more satisfactory than a slide screw tuner as far as stability and ease of operation goes. The desired signal appears then in arm 4. It is fed into a balanced mixer which receives the local oscillator power from the stabilized klystron II. The output of the balanced mixer is then fed through the IF amplifier, detector, audio amplifier and lock-in detector. The circuits of each of those components is fairly standard and will not be dwelled upon further. The microwave power is measured in arm 2 of the magic T. The power reflected from the cavity is also monitored in arm 2. This is of great help in finding the cavity when klystron I is swept in frequency by means of a sawtooth voltage on its reflector. Since the klystron mode itself might have some dips in it, (which might be mistaken for the cavity), it proved helpful to display on the scope the klystron mode simultaneously with the reflected power

from the cavity. This also provides a convenient way to measure the Q_0 of the cavity.[12] The frequency is measured roughly by means of a cavity frequency meter and more precisely by means of a transfer oscillator and high speed counter. The magnetic field is measured by means of a nuclear magnetic resonance set-up, its frequency being measured on the same counter as the microwave frequency. The nuclear resonance signal is recorded on the same trace as the electron resonance signal. Thus if the magnetic field is homogeneous enough, the nuclear sample will see the same field as the electronic sample and g-values can be conveniently determined to the accuracy of the nuclear moment (this also assumes that the signal is large enough, so that no additional error is introduced in determining the exact location of the resonance.) The field modulation coils are mounted on the pole faces and are energized by a 50-watt power amplifier. A field of 50 oersteds p.t.p. is available at 1,000 cps and a slightly higher field at 100 cps.

The magnet is a Verian 12″ modified so that it can rotate around an axis perpendicular to H_0. This was done mainly in order to make anistropy measurements more convenient. This enables one to make quick saturation measurements in isotropic materials without having to change the incident RF power. This is accomplished by rotating the magnetic field and measuring the signal strength versus angle. Since only the RF field perpendicular to the dc field causes transitions, the signal in an unsaturated isotropic sample should go as $\cos^2 \theta$; where θ is the angle between H_1 and H_0. From the deviation from this dependence, the saturation parameter can be found. This could also be done by rotating the cavity, but at microwaves is not as easy as rotating the field.

VII. A NOTE ON THE EFFECTIVE BANDWIDTH

There seems to be some confusion as to how narrow one should make an audio amplifier preceding a phase sensitive detector (lock-in) or why the band width of the IF amplifier doesn't enter in a superhet scheme. Those and similar questions have to do with the effective band width of the system $\Delta\nu$ which appears in (26). Since similar questions have been rigorously analyzed by other authors,[13, 14] the present discussion will try to stress some of the physical ideas underlying the different detection schemes.

We consider first the simple scheme illustrated in Fig. 11. It consists of an amplifier with band width $\Delta\nu_1$ centered around ν_1 followed by a phase sensitive detector with a reference voltage at V_1. The output of the phase sensitive detector has an RC filter of band width $\Delta\nu_2$. One can see that in such a system the only noise components centered around

ν_1 (this being also the reference frequency) in a band width $\Delta\nu_2$ will contribute to the output noise. This is because the beat between 2 noise components like ν_n and ν_m (see Fig. 11) is too far removed from ν_1 to produce an output voltage. (This statement implies the condition that $\Delta\nu_1 < \nu_1$ otherwise the beat between $2\nu_1$ and ν_1 could come through.) Thus in this system the band width of the amplifier is immaterial as long as the noise voltages are not so large as to saturate it.

A more serious situation may arise in the absence of a reference voltage. In this case the noise components within the band width $\Delta\nu_1$ can beat with each other and produce a noise output which would increase with the band width. This could become especially detrimental in a superheterodyne scheme in which the IF band width can be a million times larger than the output band width. It can be shown, however, that if the carrier voltage V_c at the output of the IF is large enough the IF bandwidth ΔF_{IF} does not enter into the noise consideration[13] the criterion essentially is that

$$V_c^2 > G^2 2kTZ\Delta F_{IF} \tag{60}$$

where G is the IF amplifier gain, and Z the input impedance. Condition (60) means that we want the noise which beats with the carrier to be greater than the beat between 2 noise terms. Since the former is proportional to the carrier, its predominance can be easily ascertained experimentally by increasing the IF carrier and noting whether the noise output increases proportionally. If it does, (60) is fulfilled.

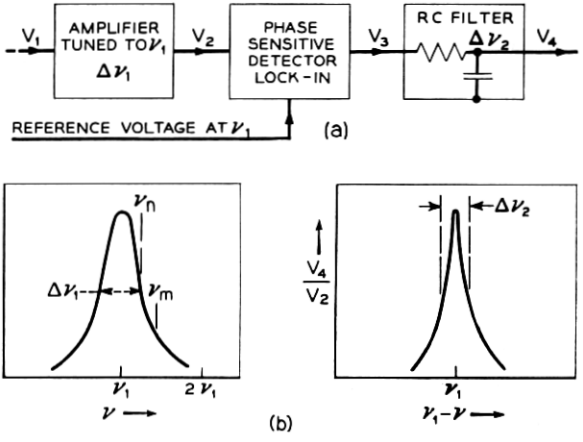

Fig. 11 — Effective band width of a phase sensitive detector $\Delta\nu_{eff} = \Delta\nu_2$. Note that the band width of the amplifier does not enter as long as $\Delta\nu_1 < \nu_1$.

In order to see what maximum gain G (60) imposes on a typical system we assume $\Delta F_{IF} = 5 \times 10^6$ c.p.sec. $Z = 10^3\Omega$; $V_c \simeq 1$V. Under those conditions we get from (60) that G has to be smaller than approximately 10^5. If on the other hand G is very small the signal level at the audio amplifier input is so low that the flicker noise of the detector can still come in. A good practical figure for the IF amplifier gain is around 60 db.

VIII. SATURATION EFFECTS

In all the previous considerations RF power saturation effects were neglected, i.e., we have assumed that the power absorbed is proportional to H_1^2, where H_1 is the RF magnetic field. When this assumption is no longer satisfied, the question of sensitivity has to be re-examined for different degrees of saturation. However it is difficult from an experimental point of view to change the conditions of the experiment for each degree of saturation and therefore an elaborate analysis of this case does not seem to be warranted. However it might be of interest to see the effect on the in phase component of the signal at complete or nearly complete saturation

The change in output voltage for a reflection cavity is (15)

$$\Delta V = \sqrt{2}\, V \frac{R_0 n^2}{(R_0 n^2 + r)^2} \Delta r$$

and from (4)

$$\frac{\Delta r}{r} = \frac{\Delta Q}{Q_0} = 4\pi\eta Q_0 \chi''$$

The RF magnetic field in the cavity is given by

$$H_1^2 = CQ_0(1 - \Gamma^2)P_{in} \tag{71}$$

where C is a constant dependent on the geometry of the cavity the reflection coefficient. Assuming a simple homogeneous saturation behaviour we substitute for χ'' the saturated value of χ_s''[1].

$$\chi_s'' = \frac{\chi_u''}{1 + \gamma_1^2 H_1^2 T_1 T_2} = \frac{\chi_u''}{1 + \gamma_1^2 T_1 T_2 C Q_0 (1 - \Gamma^2) P_{in}} \tag{72}$$

where χ_u'' is the unsaturated value of the susceptibility and P_{in} the power from the microwave source.

$$\frac{\Delta r}{r} = 4\pi\eta Q_0 \frac{\chi_u''}{1 + \gamma_1^2 T_1 T_2 Q_0 (1 - \Gamma^2) P_{in}} \tag{73}$$

and the output voltage ΔV.

$$\Delta V = \sqrt{2}\ V_0 \frac{R_0 n^2}{(R_0 n^2 + r)^2} r 4\pi\eta Q_0 \frac{\chi_u''}{1 + \gamma_1^2 T_1 T_2 C Q_0 (1 - \Gamma^2) P_{in}} \quad (74)$$

For a high degree of saturation

$$\gamma_1^2 T_1 T_2 C Q_0 (1 - \Gamma^2) P_{in} \gg 1$$

and substituting for

$$\Gamma = \frac{\frac{R_0 n^2}{r} - 1}{\frac{R_0 n_2}{r} + 1}$$

we get:

$$\Delta V = \frac{\sqrt{2}\ V_0 \pi\eta\ \chi_u''}{P_{in} \gamma_1^2 T_1 T_2 C} \quad (75)$$

The above relation shows that under saturated conditions the Q of the cavity does not enter and one might as well not use one or use a very much overcoupled cavity. This is one of the reasons why in microwave gas spectroscopy,* where lines are easier saturated a cavity is not used. (The more important reason is that in most cases one sweeps the frequency of the source, so that a cavity is difficult to use.)

Equation (75) also shows that the signal and also signal to noise goes down with increasing RF power. The above argument does not hold for the out-of-phase (dispersion) signal, in particular it breaks down completely for signals observed under fast adiabatic passage conditions.[1] For the latter case one wants as high an RF field as possible.

IX. ACKNOWLEDGEMENT

I profited greatly from discussions with various members of the resonance group at the University of California in particular with Profs. A. F. Kip, and A. M. Portis and at Bell Telephone Laboratories with Drs. R. C. Fletcher and S. Geschwind. I would like especially to thank E. Gere for his expert help in the construction of the equipment and to Prof. C. P. Slichter and Dr. R. H. Silsbee for helpful criticism of the manuscript.

REFERENCES

1. See for example F. Bloch, Phys. Rev., **70**, p. 460, 1946. N. Bloembergen, E. M. Purcell, R. V. Pound, Phys. Rev., **73**, p. 679, 1948.

* In microwave gas spectroscopy the fractional power loss per unit length α is used. Its relation to the susceptibility is $\alpha = 8_\pi\ 2\chi''/\lambda_G$ where λ_G is the guide wavelength.

2. Montgomery, Technique of Microwave Measurements, Rad. Lab. Series, No. 11.
3. C. H. Townes and S. Geschwind, J.A.P., **19,** p. 795, Aug., 1948.
4. Hamilton, Knipp and Kupper, Klystrons and Microwave Triodes. McGraw Hill, 1948, Rad. Lab. Series No. 6, p. 475.
5. Torrey, H. C. and Whitmer, C. A., Crystal Rectifiers, Rad. Lab. Series, Vol. 15, McGraw Hill, 1947.
6. M. W. P. Strandberg, H. R. Johnson, J. R. Eshbach, R.S.I., **25,** pp. 776–792, Aug., 1954.
7. Townes and Schawlow, Microwave Spectroscopy, McGraw Hill, 1955.
8. Miller, P. H., Noise Spectrum of Crystal Rectifiers, Proc. I.R.E., **35,** p. 252, 1947.
9. G. R. Nicoll, Noise in Silicon Microwave Diodes, Proc. I.E.E., **101,** pp. 317–29, Sept., 1954.
10. See for example K. Holbach, Helv. Physica Acta, **27,** p. 259, 1954; A. M. Portis, Phys. Rev., **100,** p. 1219, 1955.
11. Pound, R. V., Microwave Mixers, M.I.T. Radiation Lab. Series 16, McGraw Hill.
12. E. D. Reed, Proceedings of the National Electronics Conference, **7,** p 162, 1951.
13. S. O. Rice, B.S.T.J., **23,** pp. 282–332; B.S.T.J., **24,** pp. 46–156, 1945.
14. A. van der Ziel, Noise, Prentice Hall, Inc., 1954.